

## The Addressing of Distributed FBG Based on FMCW

Li Shou-duo<sup>1</sup>, Xiong Yan-ling<sup>1,2</sup>, Yang Wen-long<sup>1</sup> and Li Qiao-yi<sup>1</sup>

<sup>1</sup>College of Applied Science, Harbin University of Science and Technology,  
Harbin, China

<sup>2</sup>Key Laboratory of Engineering Dielectric and Its Application, Ministry of  
Education, Harbin, 150080  
xyling1964@163.com

### Abstract

*The addressing principle of distributed optical fiber Bragg grating (FBG) sensor based on frequency modulation continuous wave (FMCW) multiplexing technology was studied, and the theoretical analysis of FBG multiplex distance were carried out; In order to analyze the impact on the spectrum signal, the effect of grating position information, scanning time and scanning frequency range on the spectrum signals were analyzed by simulation. When the FBG multiplex distance is integer or non-integer multiple of system minimum resolution distance, for the FMCW multiplexing scheme was simulated. The grating distance, the scan time and the scanning frequency range significantly affect the signal strength and the signal-to-noise ratio. Finally, the related experimental system was established and the results are consistent with the theory.*

**Keywords:** FMCW; FBG; multiplex distance

### 1. Introduction

Fiber Bragg grating (FBG) has broad application prospects in optical fiber communication and optical sensing field, because of its many unique advantages [1]. As a sensing element, FBG is a way to obtain sensor information through external physical parameters controlling the modulation of fiber Bragg wavelength. So, it is a wavelength modulation type optical fiber sensor. It has easy constitutes sensor networks, wavelength coding, and other unique advantages. It can be constituted by multiplexing a distributed sensor network, in order to achieve multi-point measurement. It does this by arranging a plurality of sensors on a single optical fiber, optical fiber distribution field can be measured. Fiber is both the sensor and the information transfer channel. This eliminates the need to form additional lead measuring system, thus, reduces the complexity of the system, saves system components and operating costs. In the field of safety monitoring of large structures (such as dams, bridges, buildings and aircraft, etc.), it has broad application prospects. Especially in the smart skin structure, the use of the distributed optical fiber sensor measurement system is almost the only choice. Therefore, FBG demodulation and multiplexing become a hot research point recently years.

There are wavelength division multiplexing, spatial division multiplexing, time division multiplexing, frequency-modulated continuous wave, hybrid multiplexing [2-5] and so on. The multiplexing capability of wavelength division multiplexing is limited by the bandwidth of the light source and the maximum central wavelength drift; In practice, the signal to noise ratio of time division multiplexing technology will continue to fall with the increasing number of grating sensor; The multiplexing capability of spatial division multiplexing is not strong, because of its light lower utilization. Wherein the bandwidth of the modulated signal and the relative positions of the FBG sensor determines the number of FBG sensors that can

multiplexed by the FMCW [6-10]. Therefore, the number of multiplexed network is considerable.

## 2. Principle

### 2.1. Basic principle of FMCW multiplexing

The frequency of the voltage controlled oscillator (VCO) changes in accordance with the linear sawtooth or triangular wave. After modulated by VCO, the frequency of light source intensity will change in accordance with the linear sawtooth or triangular wave. The electric voltage signal, which is converted from the light signal reflected back by the FBG sensor by the detector, was multiplied by the original modulation signal. Difference frequency generates due to signal delay of the two multiplied signals. The position of the probe in the sensor channel can be distinguished by the difference signal. Because different sensor gratings of different channels have different delays, and different delays corresponding to different difference signals.

If VCO is an ideal linear device, the instantaneous voltage value of the transmitted signal could be written as

$$V_T(t) = V_T \cos(2\pi f_0 t + \frac{\pi B t^2}{T} + \varphi_0), 0 \leq t < T \quad (1)$$

where  $V_T$  is the amplitude of the transmitted signal,  $f_0$  is the initial frequency of the transmitted signal,  $B$  is the frequency variable width of the transmitted signal,  $T$  is the repetition period,  $\varphi_0$  is the initial phase of the transmitted signal. Figure 1 shows the basic principle of FMCW multiplexing:

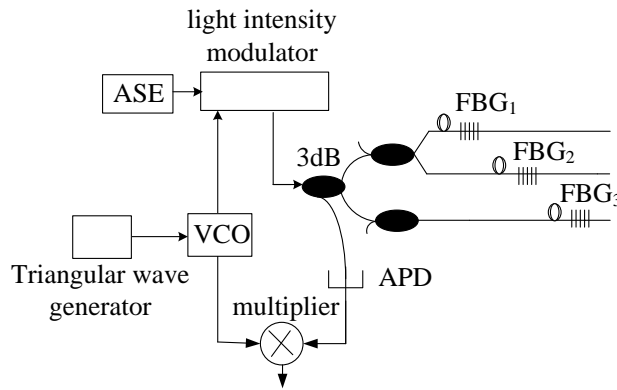


**Figure 1. Schematic of FMCW Multiplexing System**

After returning from the FBG transmission signal, the instantaneous voltage value of the echo signal is

$$V_R(t) = V_R \cos[2\pi f_0(t - \Delta t) + \frac{\pi B(t - \Delta t)^2}{T} + \varphi_0], \Delta t \leq t < T \quad (2)$$

where  $V_R$  is the amplitude of the echo signal.

Echo signal is multiplied with the original transmitted signal, then

$$V(t) = V_T(t)V_R(t)$$

$$= \frac{1}{2} V_T V_R \left\{ \cos \left[ 2\pi f_0 (2t - \Delta t) + \pi B \frac{t^2 + (t - \Delta t)^2}{T} + 2\varphi_0 \right] + \cos \left( \pi B \frac{2t\Delta t}{T} + \varphi \right) \right\}$$

where  $\varphi = 2\pi f_0 \Delta t - \pi B \frac{\Delta t^2}{T}$ ,  $\varphi$  is a stabilizing amount of the time-independent. Filter out high frequency components, then

$$V(t) = V \cos \left( \pi B \frac{2t\Delta t}{T} + \varphi \right) \quad (3)$$

The frequency is 
$$\Delta f = \frac{B\Delta t}{T} = \frac{B}{T} \frac{2nl}{c} \quad (4)$$

From the above equation, when the echo signal is multiplied by the transmitted signal, it will generate a signal whose frequency is only the location of the grating. Therefore, we can obtain the location of the grating, by detecting the frequency of the signal.

### 2.2. Analysis of Multiplex distance FBG

When the transmitting signal is at the lowest point, delayed signal remains at a frequency near the high point. At the end of time  $\Delta t$ , the difference frequencies produce a jump, as shown in Figure 2:

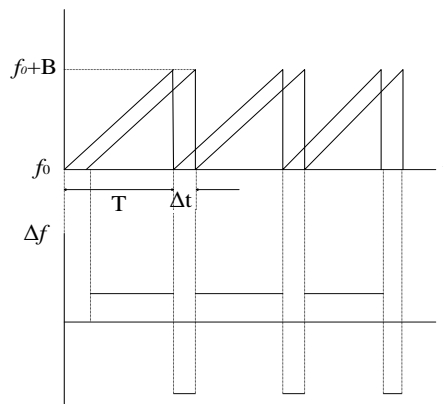


**Figure 2. Offset Frequency Figure**

The figure shows that difference frequency is not continuous. In practical applications, at the end of the time  $\Delta t$ , the difference frequency hopping will have some impact on the frequency analysis. Therefore, transition time should be met:

$$\Delta t_i = \frac{2nl_i}{c} < T \quad (5)$$

Scilicet 
$$l_i < \frac{cT}{2n} \quad (6)$$

In addition, in a ramp sweep cycle  $T$ , the number of poor signal should be complete, in order to properly addressing FBG.

Scilicet 
$$\Delta f_i T = \frac{2nBl_i}{cT} T = N \text{ Where } N = 1, 2, 3 \dots$$

Scilicet 
$$l_i = N \frac{c}{2nB}, N=1, 2, 3 \dots \quad (7)$$

### 3. Simulation

#### 3.1. The Influence Factors of Difference Frequency Signals

Simulation model was established by MATLAB / Simulink software. The returning signal was studied in the model with time delay modules. Spectrum analysis is shown in Figure 3, when  $B = 5 \text{ MHz}$ ,  $n = 1.5$ , the scan period  $T$  are taken as  $0.0025 \text{ s}$ ,  $0.005 \text{ s}$ . As can be seen from Figure 3, the larger the value of  $N$  (the farther the grating distance), then the greater the delay, the smaller the signal strength; the larger the scan cycle, then the greater the signal intensity with respect to the noise strength, the greater the signal-to-noise ratio (SNR).

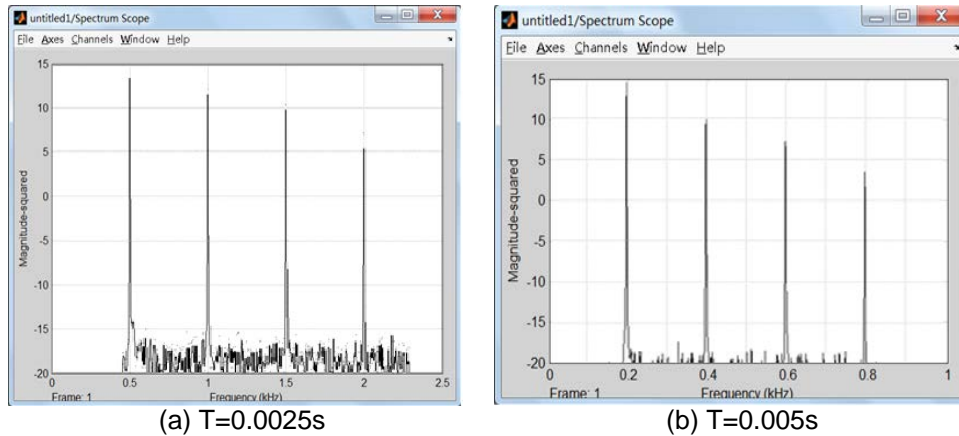


Figure 3. Spectrum Analysis of Different Scanning Cycle

Spectrum analysis is shown in Figure 4, when  $T = 0.05 \text{ s}$ ,  $n = 1.5$ ,  $B$  are taken as  $5 \text{ M}$ ,  $10 \text{ M}$ . As can be seen from Figure 4, the smaller scanning frequency range, then the greater the signal intensity with respect to the noise strength, the greater the SNR. But, it can be seen from the spatial resolution formula (7), wherein  $N=1$ , the smaller the scanning frequency, and the greater value of  $\Delta l$ . Therefore, in the practical application, not a scanning range as small as possible, it should be processed as appropriate according to the actual situation.

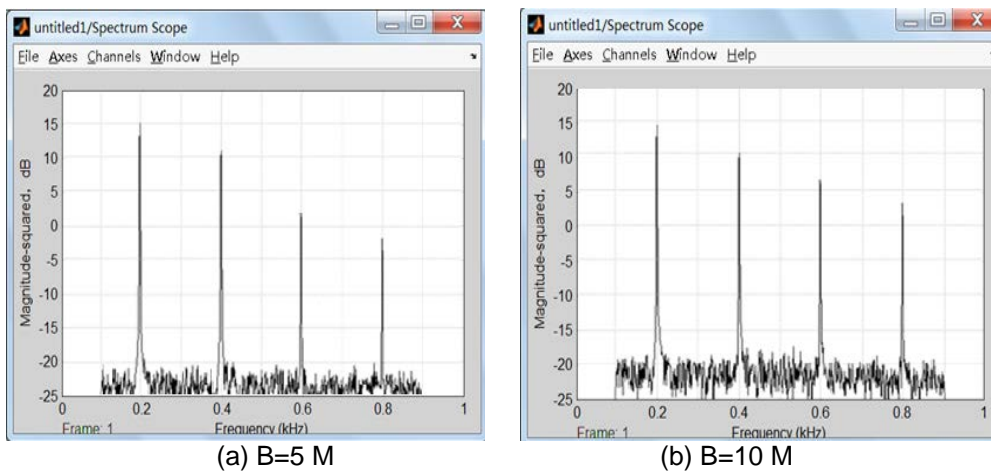
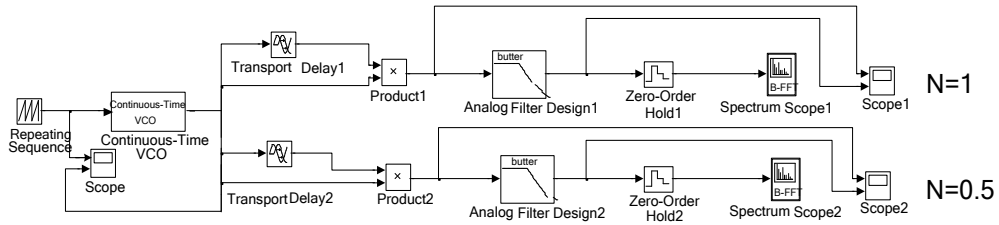


Figure 4. Spectrum Analysis of Different Scanning Frequency Range

### 3.2. Simulation of FBG Multiplex Distances



**Figure 5. Simulation Diagram on Exploring FBG Multiplex Distance**

The simulation system was established by the Simulink of the MATLAB software, as shown in Figure 5. Signal frequency parameter output by the VCO is  $T=0.01$  s,  $B=1$  MHz, when the distance of the selected raster are 100 m, 50 m, system satisfies formula (6). We calculated, the complete waveform numbers of difference frequency signal were  $N=1, 0.5$  in a single cycle, the resulting simulation waveforms and spectrum are shown in Figure 6 to Figure 7:

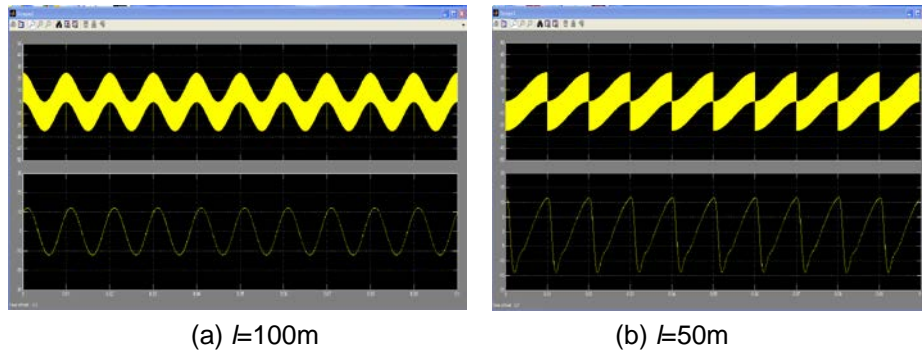


**Figure 6. Waveform before Filtering and after Filtering**

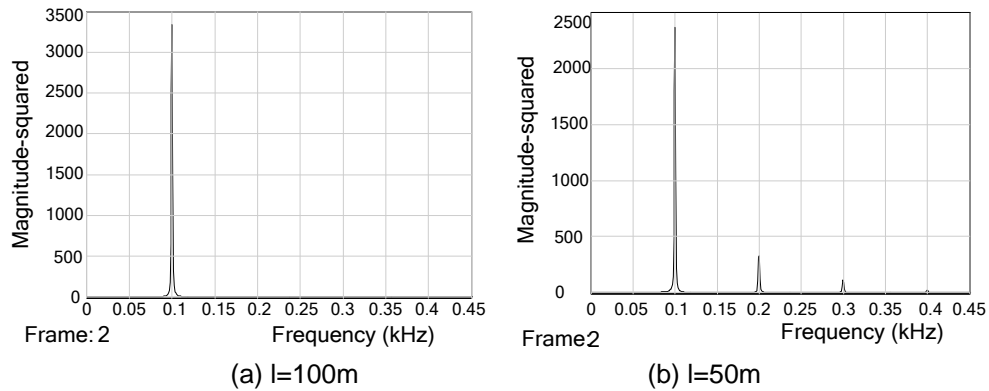


**Figure 7. Spectrum of Different Frequencies**

As shown in Figure 6a and Figure 7a, when  $l_1=100$  m, the number of full difference frequency signal is  $N=1$  in a scan cycle. After filtering through the filter, the difference frequency signal is extracted. We can see from Figure 7a, difference frequency signal only contains a unique frequency of 100 Hz, and the difference frequency is 100 Hz in theory.

Therefore, the simulation results and theoretical results are consistent. That is, the position information of the FBG can be obtained by differential frequency information, so as to achieve the purpose of addressing the FBG.

As can be seen from the Figure 6b and Figure 7b, a half complete difference frequency signal appears in one scanning periods when  $l_2=500$  m. Since the mixing signal output of multiplier jump at the end of each period, the envelope of the extracted signal produce a certain distortion after the output is filtered by the filter. According to Figure 7b we can see that difference frequency signal contains a variety of frequency information, 100 Hz, 200 Hz, 300 Hz respectively. Namely, there will be multiple frequencies when a FBG is demodulated by the system. But the difference frequency should be 50 Hz by calculated theoretically. Therefore, it can't achieve the purposes of FBG addressing due to the simulation results and theoretical results are inconsistent.

So, in order to address correctly in the FBG multiplexing system, FBG's location should meet formula (7) as much as possible. In order to understand the impact of the results when the grating distance does not meet formula (7), the selected grating structures simulation system was shown in Figure 8:

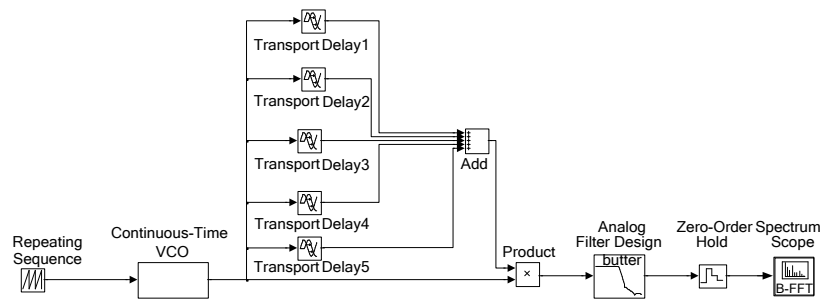


**Figure 8. FMCW Technology Simulation System**

In the system, the output signal frequency of voltage controlled oscillator meet  $T=0.001$  s,  $B=1000000$  Hz; the grating distances are  $l_1=100$  m,  $l_2=120$  m,  $l_3=150$  m,  $l_4=400$  m,  $l_5=500$  m, respectively;  $N=1, 1.2, 1.5, 4, 5$ , and satisfy formula (6). The resulting simulation results are shown in Figure 9.

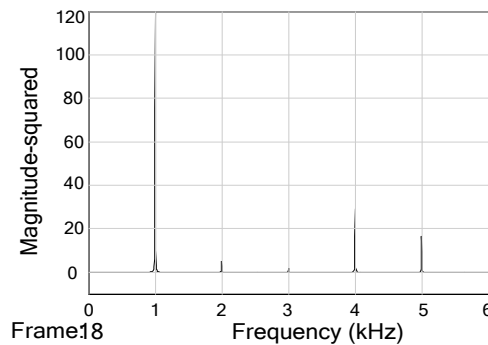


**Figure 9. Simulation Spectrum when N = 1,1.2,1.5,4,5**

The minimum resolution distance of the system is 100 m, from the theoretical calculation, the distance of the grating, 100 m, 120 m, 150 m, 400 m, 500 m, corresponds to difference frequency, 1000 Hz, 1200 Hz, 1500 Hz, 4000 Hz, 5000 Hz, respectively. However, Figure 9

shows the resulting frequency is mainly distributed at the 1000 Hz, 4000 Hz, 5000 Hz, without the characteristic frequency of 1200 Hz and 1500 Hz corresponding to the grating distance 120 m and 150 m. Because the portion of difference frequency signal corresponding to the grating distance of 120 m and 150 m is coupled to it, the power of 1000 Hz was significantly higher than 4000 Hz and 5000 Hz. Therefore, the purpose of addressing can't achieve when multiplex distances of the FBG system are the non-integer multiple of minimum resolution distance; only when multiplex distances of the FBG system are the non-integer multiple of minimum resolution distance.

## 4. Experimental Study

The experimental system was established, and triangular wave generator and VCO, as shown in Figure 1, were instead by the arbitrary waveform generator. The signals with difference frequency were detected by a digital lock-in amplifier.

### 4.1. Multiplex Distances of the FBG System are the Non-Integer Multiple of Minimum Resolution Distance

The minimum resolution distance is 100 m, which is calculated according to formula (7), wherein  $B=1$  MHz,  $T=32.3$  ms,  $n=1.5$  and  $N$  was set to 1. The multiple measurements were delivered when the  $l$  were taken 1000 m, 1050 m and 1100 m. The experimental difference frequencies are 330.4 Hz and 360.4 Hz, which are consistent with the theoretical values 310 Hz and 340.6 Hz when the multiplex distances  $l$  of the FBG are 1000 m and 1100 m, respectively. The differences between the experimental and theoretical values were caused by the time delay of the passive devices in the system. It is important to point out that there are two experimental difference frequencies to one non-integer multiple of Minimum resolution distance; for example, the calculated difference frequency is 325.1 Hz, but the experimental difference frequency are 330.4 Hz and 360.4 Hz when  $l = 1050$  m. Therefore, the addressing can't be achieved when FBG system multiplex distances are the non-integer multiple of minimum resolution distance, because of the appearance of more than one frequency.

### 4.2. Multiplex Distances of the FBG System are the Integer Multiple of Minimum Resolution Distance

The minimum resolution distance is 10 m, wherein  $B=10$  MHz,  $T=32.3$  ms. The multiple measurements were delivered when the  $l$  were taken 80 m, 100 m, 1000 m, 1080 m and 1100 m. Difference frequency signal frequency of theory and grating distance of the curve, difference frequency signal frequency experimental values and grating distance of the curve are shown in Figure 10.

From the Figure 10 to know, theoretical curve fitting equation is  $\Delta f = 3.095l$  ; Experimental curve fitting equation is  $\Delta f = 3.30189l + 3.01366$ , goodness of fit is  $R^2 = 1$ . As can be seen, the experimental and theoretical  $\Delta f$  and  $l$  of the curve are basically the same. Therefore, when multiplex distances of the FBG system are the integer multiple of Minimum resolution distance, the system can achieve the FBG addressing functions.

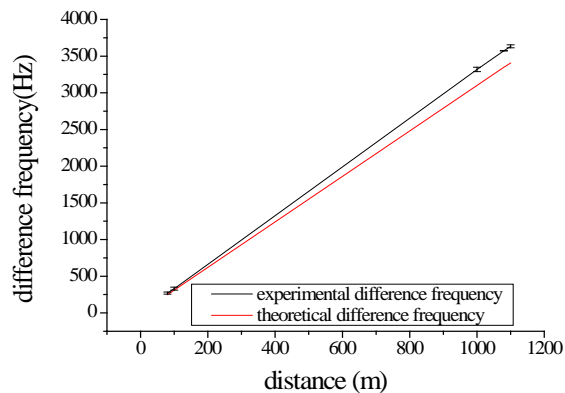


Figure 10. The Relationship between of  $\Delta f$  and  $l$

## 5. Conclusion

Based on the basic principle of FMCW technology, the requirement of FBG multiplex distances were studied, and the results shows that the purpose of addressing can be achieved only when FBG system multiplex distances are the integer multiple of minimum resolution distance. The FMCW simulation system based on MATLAB/Simulink was established, the simulation results shows that the larger the value of  $N$  (the farther the grating distance), the greater the delay, and then the smaller the signal strength; the larger the scan cycle, the smaller scanning frequency range, then the greater the signal intensity with respect to the noise strength, the greater the SNR. And the multiplex distances of the FBG were investigated. The FBG sensor network meeting the requirements of multiplex distance FBG and not meeting the requirements of multiplex distance FBG were stimulated and discussed. The obtained results are consistent with the theory. The experimental system was set up, which verify that the purpose of addressing can't be achieved when FBG system multiplex distances are the non-integer multiple of minimum resolution distance. Only when FBG system multiplex distances are the integer multiple of minimum resolution distance, the system can achieve the FBG addressing functions.

## Acknowledgment

This work was financially supported by the Natural Science Foundation of Heilongjiang Province of China (F201131), the Graduate innovative research projects of Heilongjiang Province (Y00030).

## References

- [1] K. O. Hill, B. Malo and F. Bilodeau, Applied Physics Letters, vol. 62, no. 10, (1993).
- [2] J. J. Bai, Y. Wu and C. Y. Ran, "Acta Optica Sinica", vol. 29, no. 2, (2009).
- [3] F. Ito, X. Y. Fan and Y. Koshikiya, Journal of Lightwave Technology, vol. 30, no. 8, (2012).
- [4] N. Hu, Transportation Science & Technology, vol. 3, (2009).
- [5] W. W. Fang, D. S. Jiang and C. Zhang, Optics & Optoelectronic Technology, vol. 2, no. 5, (2004).
- [6] F. C. Teng, G. Yang and B. Dong, Chinese Journal of Sensors and Actuators, vol. 23, no. 12, (2010).
- [7] R. A. Perez, O. Frazão and J. L. Santos, IEEE Sensors Journal, vol. 9, no. 12, (2009).
- [8] Y. L. Yu, H. Y. Tan and Y. K. Zhong, Chinese Journal of Lasers, vol. 27, no. 12, (2000).
- [9] K. C. Peter, C. J. Chan and J. Wei, IEEE of Selected Topics in Quantum Electronics, vol. 6, no. 5, (2000).
- [10] Z. Q. Li, L. J. Huang and F. Wu, Optical Technique, vol. 30, no. 2, (2004).